A hydroxyphenyloxadiazole lithium complex as a highly efficient blue emitter and interface material in organic light-emitting diodes

Fushun Liang, Jiangshan Chen, Lixiang Wang,* Dongge Ma, Xiabin Jing and Fosong Wang

State Key Laboratory of Polymer Physics and Chemistry, Changchun Institute of Applied Chemistry, Chinese Academy of Sciences, Changchun 130022, People's Republic of China. E-mail: lixiang@ciac.jl.cn; Fax: +86-431-5685653; Tel: +86-431-5694787

We synthesized a hydroxyphenyloxadiazole lithium complex (LiOXD) as a blue light-emitting and electron injection/transport material to be used in double-layer organic electroluminescent devices. Devices with the concise configuration of ITO/TPD/LiOXD/Al showed bright blue EL emission centered at 468 nm with a maximum luminance of 2900 cd m^{-2}. A current efficiency of 3.9 cd A^{-1} and power efficiency of 1.1 lm W^{-1} were obtained. LiOXD was also examined as an interface material. The efficiency of an ITO/NPB/Alq$_3$/Al device increased considerably when LiOXD was inserted between Alq$_3$ and aluminium. The improvement of the device characteristics with LiOXD approached that observed with the dielectric LiF salt.

Introduction

Organic light-emitting diodes (OLEDs) are of growing interest in display applications because they are able to emit colors throughout the visible spectrum and with high luminous efficiency. There have been extensive studies on using low molecular weight complexes to make organic electroluminescent (EL) devices with the aim of achieving high brightness, multicolor emission, improving the durability, and efficiency.[1–6] Among RGB full color emission blue light emission is hard to produce due to its intrinsic characteristic of having a wide bandgap. Furthermore, the large bandgap energy may block injection of electrons from the cathode. As a result, blue emitters often have lower efficiency than red and green light-emitting materials. To date high performance blue light-emitting diodes including metal complexes and small organic molecules reported in the literature were usually realized by multiple-layer devices, at least triple-layer devices.[7] From this we can see that the device fabrication is relatively complicated, so there is a need to further develop blue light-emitting materials and simultaneously simplify device structures. In the past few years our group has been concentrating on developing highly efficient small organic molecules-based electroluminescent devices with simple device configurations.[8]

Recently, some *ortho*-hydroxyphenyloxadiazole complexes were proved to be good emitting materials for they possess the combined properties of metal chelates and oxadiazoles in EL applications,[9,10] because oxadiazole derivatives themselves are among the widely used electron-transporting materials.[11,12] In the present paper this ligand was still adopted and a lithium compound 2-(5-phenyl-1,3,4-oxadiazolyl)phenolatolithium (LiOXD) was synthesized. The selection of elemental lithium as the central ion is based on the following considerations: (i) it has been reported that some lithium metal complexes such as 2-(2-hydroxyphenyl)benzoxalatolithium, 8-hydroxyquinolinolato-lithium (Liq) and lithium tetra(8-hydroxyquinolinolato)boron can be used as efficient emitter materials in OLEDs,[13–15] (ii) to meet the need for pure blue light emission, and (iii) elemental lithium and a lithium compound have been demonstrated to improve electron injection and to enhance electroluminescent efficiency.[16,17] In our experiment the explored lithium complex was found to be a good blue light-emitting material, and can

also function as an interface material like the effect of the dielectric salt LiF.

Experimental

General procedures

Only analytical grade quality chemicals were used. The starting materials were purchased from Beijing Chemical Co. and used without further purification. ^{1}H NMR was recorded on a Varian Spectrometer operating at 400 MHz. Chloroform (CDCl$_3$) and dimethylsulfoxide (DMSO-d_6) were used as solvents, and tetramethylsilane (TMS) as internal standard. C, H, N, elemental analyses were conducted with Bio-Rad Co's elemental analytical instrument. Thin-layer chromatography (TLC) was carried out on SiO$_2$ (silica gel F 254, Whatman). UV-vis absorption and photoluminescence spectra were recorded on a Varian Cray 50 spectrometer and a Perkin Elmer LS50B luminescence spectrometer, respectively. T_g and T_d of the complex were determined by DSC and TGA using Perkin-Elmer DSC-6 and TGA-7 analyzer systems, respectively. Both thermal analyses were performed with scanning (both heating and cooling) rates of 10 °C min^{-1} under nitrogen atmosphere. Cyclic voltammograms were recorded with a computer controlled EG&G Parc model 273 potentiostat/galvanostat at a constant scan rate of 100 mV s^{-1}. Measurements were performed in a conventional three-electrode cell. The working electrode was glassy carbon (diameter 0.8 mm), the counter electrode was a platinum mesh and the reference electrode was Ag/AgCl with a salt bridge containing 0.1 M tetrabutylammonium perchlorate (TBAP) in deoxygenated dry dichloromethane as the supporting electrolyte.

Syntheses

The synthetic route towards 2-(5-phenyl-1,3,4-oxadiazolyl)-phenolatolithium (LiOXD) is depicted in Scheme 1. The ligand 2-(5-phenyl-1,3,4-oxadiazol-yl)phenol (HOXD) was prepared according to the literature method with minor modification.[9]

Synthesis of LiOXD. To a solution of HOXD (0.476 g, 2 mmol) in 20 mL THF was added lithium hydroxide (0.084 g, 2 mmol). A white precipitate appeared after 10 min. The

DOI: 10.1039/b307209f

This journal is © The Royal Society of Chemistry 2003
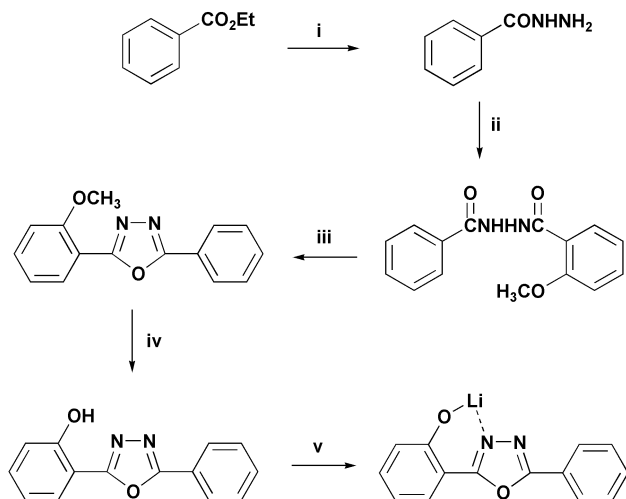
Scheme 1 Synthetic route towards LiOXD. Reagents and conditions: i, NH₂NH₂·H₂O, reflux, 24 h; ii, o-MeO-PhCOCl, Et₃N, r.t., 15 h; iii, POCl₃, 120 °C, 5 h; iv, BBr₃, CH₂Cl₂, −78 °C, 48 h; v, MOH, THF, r.t., 24 h.

solution was stirred at room temperature overnight. A white solid was collected by filtration, then washed with water and THF, and dried under vacuum to provide 0.46 g (yield 94%) of powder product. Pure LiOXD was obtained by train sublimation. m.p. 162–164 °C, ^{1}H NMR (300 MHz, CDCl₃): δ [ppm] 6.27 (t, 1 H, Ar-H), 6.48 (d, 1 H, Ar-H), 7.10 (t, 1 H, Ar-H), 7.62 (m, 3 H, Ar-H), 7.69 (d, 1 H, Ar-H), 8.09 (m, 2 H, Ar-H). MS (m/z): 244. Anal. Calcd for C₁₄H₉LiN₂O₂: C, 68.85; H, 3.69; N, 11.48. Found: C, 69.83; H, 3.61; N, 10.92%.

Device fabrication and testing. The EL devices using LiOXD as the emitting layer were fabricated on an indium-tin-oxide (ITO) substrate. The ITO glass was routinely cleaned by ultrasonic treatment in detergent solutions, followed by rinsing with acetone, boiling in isopropanol, rinsing in methanol and then in de-ionized water. The glass was dried in a vacuum oven after each cleaning step. The electroluminescent device was fabricated by high vacuum (2 × 10⁻⁶ Torr) thermal evaporation techniques. A shadow mask with 3 × 3 mm² openings was used to define the cathodes. The EL spectra were recorded with a JY-SPEX CCD-3000 V spectrometer. The current–luminance–voltage characteristics were measured using a Keithley source measurement unit with a calibrated silicon photodiode. All the measurements were performed under atmospheric conditions in unsealed vessels.

Results and discussion

Synthesis and fundamental physical properties

Scheme 1 depicted the synthetic route towards the ligand HOXD and the corresponding LiOXD. The ligand HOXD itself showed strong photoluminescence when illuminated by UV light due to its excited state intramolecular proton transfer characteristics. Its photoluminescent and electroluminescent properties have been reported previously.[18] LiOXD complex was synthesized via depronation of ligand HOXD by using lithium hydroxide (LiOH). From the ^{1}H NMR spectra we can see that after complexation the chemical shift values of LiOXD

all shift to high field compared to those of HOXD, indicating that reactions between metal ions and phenols occur. As anticipated, metal complex LiOXD displayed intense blue photoluminescence (PL) in the solid state. The fundamental optical, electrochemical and thermal properties are summarized in Table 1. In dichloromethane solution LiOXD exhibits a peak emission at 417 nm. From the electrochemical property one can see that LiOXD has a low reduction potential (E_{red} = −1.62 V vs. Fc), indicating that the LiOXD complex is beneficial for electron injection. The PL quantum efficiency is 24% in the thin film state, which makes it suitable for EL studies.

OLEDs with LiOXD as a blue emitter

To investigate its EL properties, organic electroluminescent devices based on LiOXD as the emitting and electron injection/transport layers were constructed. The device fabrication method was the same as that reported in previous literature.[8] The configurations of single- and double-layer EL devices are ITO/LiOXD (80 nm)/Al (100 nm) and ITO/TPD (50 nm)/LiOXD (50 nm)/Al (100 nm), in which TPD (N,N′-diphenyl-N,N′-bis(3-methylphenyl)-1,1′-biphenyl-4,4′-diamine) was chosen as the hole-transporting layer. Fig. 1 depicts the EL spectra corresponding to these two device structures. We can see that the EL spectrum of the double-layer device was almost identical with that of the single-layer device. The peak intensity of the EL spectra was located at 468 nm. It should be noted that the EL spectrum of the former is a little broader than that of the latter. This may be attributed to the existence of weak exciplex emission between the hole-transporting TPD layer and the light-emitting LiOXD layer.[19] A strong exciplex emission was observed when NPB (N,N′-di[naphthalenyl]-N,N′-diphenyl)(1,1′-biphenyl)-4,4′-diamine) was used as the hole-transporting layer, which resulted in the emission color of the electroluminescent device being not blue, but green. The current–voltage–luminance characteristics for single- and double-layer devices are shown in Fig. 2. In single-layer devices the maximum luminance was only 44 cd m⁻² and the turn-on voltage was as high as 12 V. When TPD was introduced as the hole-transporting layer, the devices showed dramatic improvement in EL performance compared with single-layer devices. The maximum luminance reached 2900 cd m⁻² at a drive
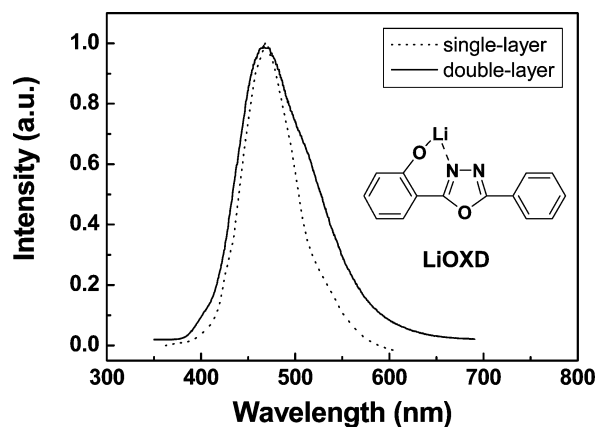

Fig. 1 EL spectra of single-layer device ITO/LiOXD/Al and double-layer device ITO/TPD/LiOXD/Al (insert: the molecular structure of LiOXD).

Table 1 Optical, electrochemical, and thermal properties of LiOXD

Compd.	Abs^a/nm	PL^a/nm	Φ_f (%)	E_{red}^b/V	HOMO^c/eV	LUMO/eV	E_g^{OPT}/eV	T_d/°C
LiOXD	230, 274, 314	417	24	−1.62	−6.34	−2.72	3.62	378

^{a}Samples were dissolved in dichloromethane (DCM) when spectra were recorded. ^{b}From CV in dichloromethane vs Ag/AgNO₃, with ferrocene (Fc) as internal standard. ^{c}Calculated from optical band gap.
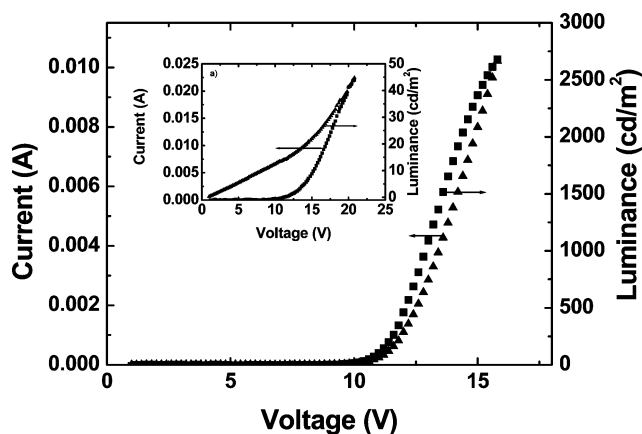
Fig. 2 The *V–I* and *V–L* characteristics of double-layer device ITO/TPD/LiOXD/Al (insert: the *V–I* and *V–L* characteristics of single-layer device ITO/LiOXD/Al).

voltage of 17 V and a current density of 0.12 A cm^{-2}. A device with a luminance of 950 cd m^{-2} at a low current density of 20 mA cm^{-2} is bright enough for practical display panel applications. A maximum current efficiency of 3.9 cd A^{-1} was obtained (see Fig. 3). The maximum luminous efficiency was estimated to be 1.1 lm W^{-1} with a luminance of 103 cd m^{-2} at the driving voltage of 11 V. The external quantum efficiency was relatively high with a value of 2.4% (corresponding to 3.5 cd A^{-1} or 0.86 lm W^{-1}) at about 20 mA cm^{-2}. The EL performance was appreciably good considering that no additional interface layers such as CuPc and LiF were employed in these devices. These values are also comparable with or higher than known electroluminescent efficiencies reported in the literature, but the device structure employed here is much more simple.[7] The impressive EL efficiency may be attributed to i) the oxadiazole segment in LiOXD has excellent electron-transporting ability and ii) the lithium salt is favorable for electron injection.

OLEDs with LiOXD as an interface material

Optimum thickness of LiOXD. The lithium complex was also examined as an interface material in double-layer devices ITO/NPB(40 nm)/Alq$_3$(60 nm)/LiOXD(*x* nm)/Al with different thicknesses of LiOXD (*x* = 1, 2, 3, 5). The a) voltage–luminance curve; b) current–luminance curve; c) current–current efficiency curve, and d) current–power efficiency curve of the devices are shown in Fig. 4. We can see from Fig. 4a and b that the luminance of the devices changes with different thicknesses of LiOXD. When the thickness is 1 nm, 2 nm, 3 nm, 5 nm, the maximum luminance is 15964 cd m^{-2}, 18389 cd m^{-2}, 14246 cd m^{-2}, and 5408 cd m^{-2}, respectively. Among them the 2 nm thickness LiOXD device is the brightest and the 5 nm thickness device is relatively poor compared to the other three devices. As shown in Fig. 4a, the four devices gave low turn-on voltages of 3.8 V, 3.0 V, 2.8 V and 3.2 V in the sequence of increasing LiOXD film thickness. Furthermore, these devices exhibit high current efficiency and power efficiency with values
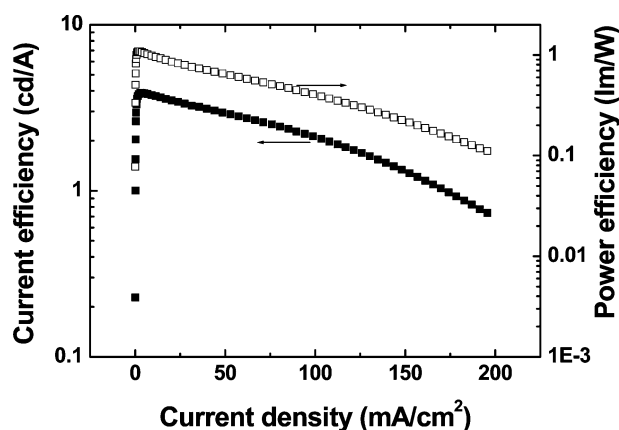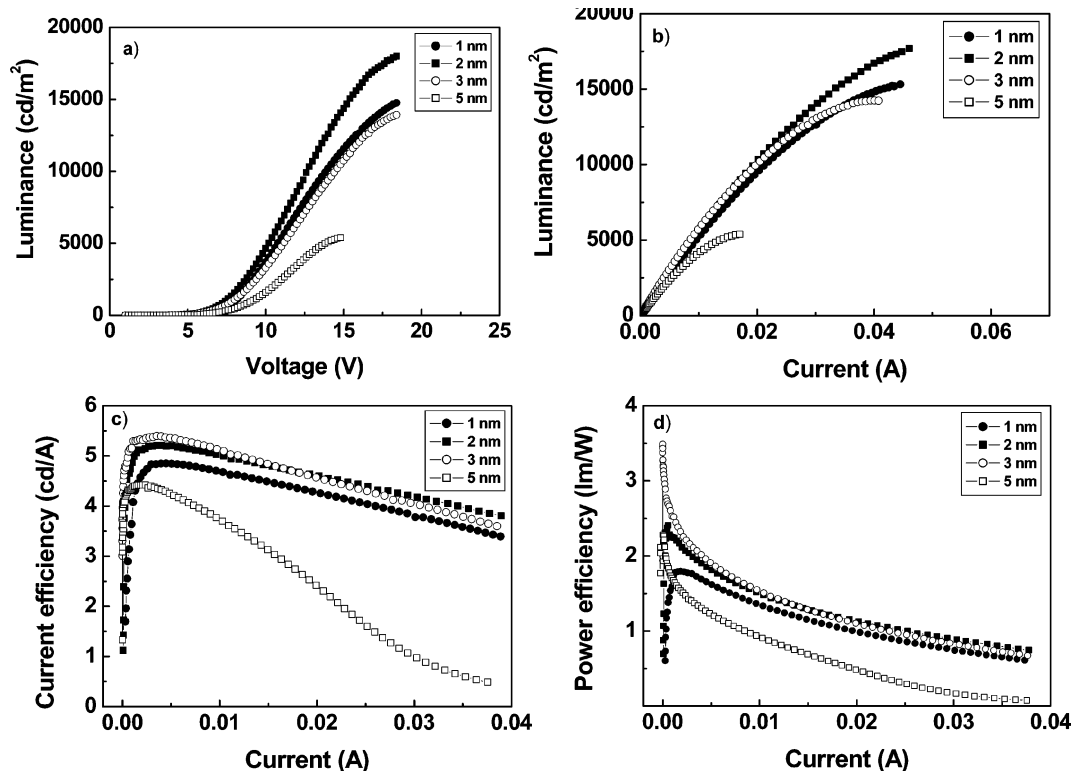

Fig. 3 The EL efficiencies as a function of current density of the double-layer device ITO/TPD/LiOXD/Al.

Fig. 4 The a) voltage–luminance curve; b) current–luminance curve; c) current–current efficiency curve, and d) current–power efficiency curve of double-layer devices ITO/NPB(40 nm)/Alq$_3$(60 nm)/LiOXD(*x* nm)/Al (*x* = 1, 2, 3, 5) with different thicknesses of LiOXD interface layer.
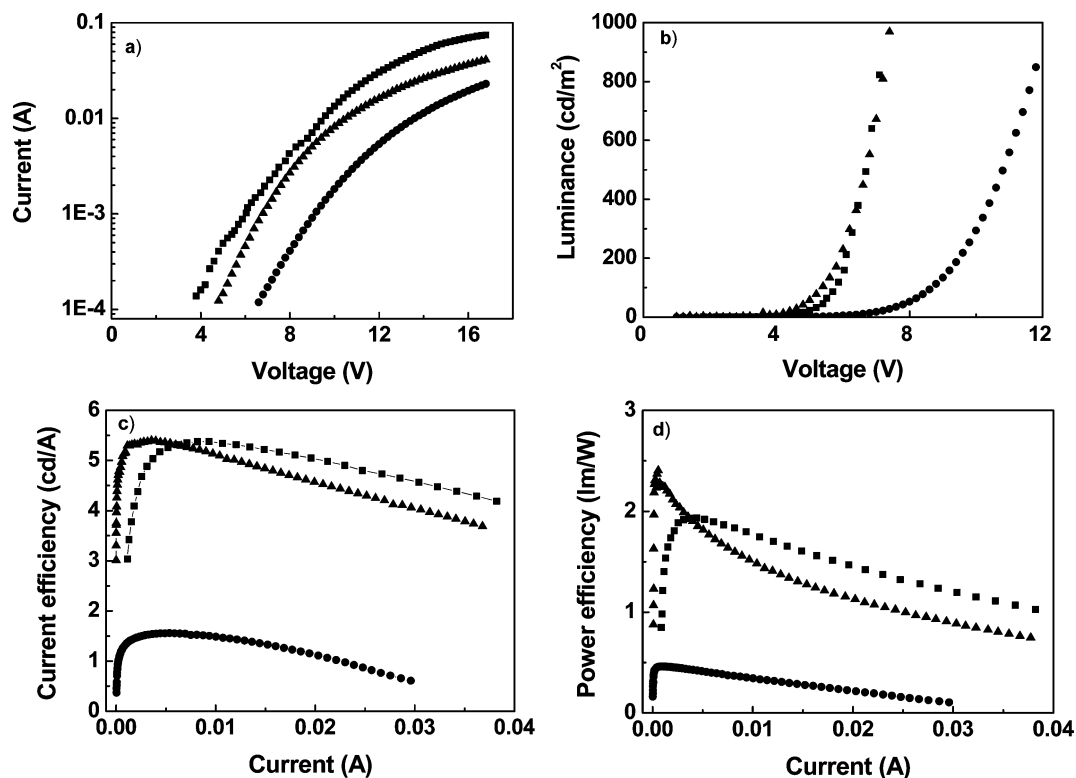
Fig. 5 The a) current–voltage curve; b) voltage–luminance curve; c) current–current efficiency curve, and d) current–power efficiency curve of double-layer devices: (●) ITO/NPB/Alq$_3$/Al; (▲) ITO/NPB/Alq$_3$/LiOXD(2 nm)/Al, and (■) ITO/NPB/Alq$_3$/LiF(1 nm)/Al.

of 4.85 cd A^{-1}, 1.80 lm W^{-1} (1 nm); 5.21 cd A^{-1}, 2.4 lm W^{-1} (2 nm); 5.6 cd A^{-1}, 3.4 lm W^{-1} (3 nm) and 4.4 cd A^{-1}, 3.0 lm W^{-1} (5 nm) [see Fig. 4c and d]. The efficiency of the 3 nm thickness device is similar to that of the 2 nm thickness device, but the stability of the 3 nm thickness device is slightly poorer than the 2 nm thickness device. Clearly the best result can be obtained from the 2 nm thickness device.

Comparison between LiOXD and LiF. To evaluate the performance of devices ITO/NPB(40 nm)/Alq$_3$(60 nm)/LiOXD(2 nm)/Al, in which LiOXD was used as an interface material, control devices ITO/NPB(40 nm)/Alq$_3$(60 nm)/Al with an Al cathode and ITO/NPB(40 nm)/Alq$_3$(60 nm)/LiF(1 nm)/Al with a LiF/Al cathode were fabricated under the same conditions for comparison purposes. The a) current–voltage curve; b) voltage–luminance curve; c) current–current efficiency curve, and d) current–power efficiency curve of the three kinds of devices are shown in Fig. 5. To achieve the same current value, the required voltage is in the order of Al device > LiOXD/Al device > LiF/Al device [see Fig. 5a]. That means the current in the reference device without any interface layer is low, while with the introduction of an interface layer, the current increases considerably, although the current of the LiOXD/Al device is a little lower than that of the LiF/Al device. Since the light output is directly proportional to the injected current, this means that the luminance of the LiOXD/Al device is not as good as that of the LiF/Al device at high driving voltage. But at low driving voltage, this is not the case, as can be seen from Fig. 5b. In particular, the maximum luminance of the LiOXD/Al device can reach up to 18520 cd m^{-2} at 20 V and the maximum luminance of the LiF/Al device can reach up to 21400 cd m^{-2} at 17 V. By contrast, the maximum luminance of the Al device is merely 2510 cd m^{-2} at 16 V.

The current efficiency and power efficiency of the LiOXD/Al device approach those of the LiF/Al device from the whole. However, at low current, the current and power efficiency of the LiOXD/Al device are higher than those of the LiF/Al device. For example, the LiOXD/Al device reached a maximum

power efficiency of 2.4 lm W^{-1} with a luminance of 300 cd m^{-2} at a voltage of 6 V. At the same current value, the maximum power efficiency of the LiF/Al device is 0.85 lm W^{-1} with a luminance of 160 cd m^{-2}. On the other hand, the device with the LiOXD interface layer shows significant improvement (3.5 times for current efficiency and 6 times for power efficiency) in EL performance compared to the reference Al device. From the above it is concluded that the EL performance when LiOXD is employed as the interface material approaches that found using dielectric LiF salt and is superior to LiF at low current density.

Conclusion

In summary, a blue light-emitting lithium–oxadiazole complex was developed. Electroluminescence results indicate that this complex is not only an excellent blue emitter with a maximum current efficiency of 3.9 cd A^{-1} and power efficiency of 1.1 lm W^{-1} in an ITO/TPD/LiOXD/Al EL device, but also a good electron injection/transport material to increase the efficiency of NPB/Alq$_3$/Al devices considerably when inserted between Alq$_3$ and the aluminium cathode. They provide potential applications in electroluminescent devices.

Acknowledgements

References

1 C. W. Tang and S. A. Van Slyke, *Appl. Phys. Lett.*, 1987, **51**, 913.
2 J. Kido and Y. Iizumi, *Chem. Lett.*, 1997, **310**, 963.
3 L. M. Leung, W. Y. Lo, S. K. So, K. M. Lee and W. K. Choi, *J. Am. Chem. Soc.*, 2000, **122**, 5640.
4 S. Tokito, K. Noda, H. Tanaka, Y. Taga and T. Tsutsui, *Synth. Met.*, 2000, **111–112**, 393.
5 J. Shi, C. H. Chen and K. P. Klubek, US Pat. Appl. 1997, **75**, 897.

6 A. Elschner, H. W. Heuer, F. Jonas, S. Kirchmeyer, R. Wehrmann and K. Wussow, *Adv. Mater.*, 2001, **13**, 1811.

7 (*a*) Y. H. Kim, D. C. Shin, S. H. Kim, C. H. Ko, H. S. Yu, Y. S. Chae and S. K. Kwon, *Adv. Mater.*, 2001, **13**, 1690; (*b*) L.-H. Chan, H.-C. Yeh and C.-T. Chen, *Adv. Mater.*, 2001, **13**, 1637; (*c*) K.-T. Wong, Y.-Y. Chien, R.-T. Chen, C.-F. Wang, Y.-T. Lin, H.-H. Chiang, P.-Y. Hsieh, C.-C. Wu, C. H. Chou, Y. O. Su, G.-H. Lee and S.-M. Peng, *J. Am. Chem. Soc.*, 2002, **124**, 11576; (*d*) L.-H. Chan, R.-H. Lee, C.-F. Hsieh and H.-C. Yeh, *J. Am. Chem. Soc.*, 2002, **124**, 6469; (*e*) Y. T. Tao, C. H. Chuen, C. W. Ko and J. W. Peng, *Chem. Mater.*, 2002, **14**, 4256; (*f*) H.-T. Shih, C.-H. Lin, H.-H. Shih and C.-H. Cheng, *Adv. Mater.*, 2002, **14**, 1409.

8 (*a*) F. S. Liang, Z. Y. Xie, L. X. Wang, X. B. Jing and F. S. Wang, *Tetrahedron Lett.*, 2002, **43**, 3427; (*b*) G. Wang, F. S. Liang, Z. Y. Xie, G. P. Su, L. X. Wang, X. B. Jing and F. S. Wang, *Synth. Met.*, 2002, **131**, 1; (*c*) F. S. Liang, J. S. Chen, Y. X. Cheng, L. X. Wang, D. G. Ma, X. B. Jing and F. S. Wang, *J. Mater. Chem.*, 2003, **13**, 1392; (*d*) F. S. Liang, Q. G. Zhou, L. X. Wang, D. G. Ma, X. B. Jing and F. S. Wang, *Chem. Mater.*, 2003, **15**, 1935.

9 J. F. Wang, G. E. J. Jabbour, E. A. Mash, Jeff Anderson, Y. D. Zhang and P. A. Lee, *Adv. Mater.*, 1999, **11**, 1266.

10 N. X. Hu, M. Esteghamatian, S. Xie, Z. Popovic, Ah-Mee. Hor, B. Ong and S. N. Wang, *Adv. Mater.*, 1999, **11**, 1460.

11 C. Adachi, T. Tsutui and S. Saito, *Appl. Phys. Lett.*, 1990, **56**, 799.

12 H. Antoniadis, M. Inbasekaran and E. P. Woo, *Appl. Phys. Lett.*, 1998, **73**, 3055.

13 Y. Kim, J-G. Lee and S. Kim, *Adv. Mater.*, 1999, **11**, 1463.

14 C. Schmitz, H.-W. Schmidt and M. Thelakkat, *Chem. Mater.*, 2000, **12**, 3012.

15 X. T. Tao, H. Suzuki, T. Wada, S. Miyata and H. Sasabe, *J. Am. Chem. Soc.*, 1999, **121**, 9447.

16 E. I. Haskal, A. Curioni, P. F. Seidler and W. Andreoni, *Appl. Phys. Lett.*, 1997, **71**, 1151.

17 L. S. Hung and C. W. Tang, *Appl. Phys. Lett.*, 1999, **74**, 3209.

18 F. S. Liang, L. X. Wang, D. G. Ma, X. B. Jing and F. S. Wang, *Appl. Phys. Lett.*, 2002, **81**, 4.

19 J. Thompson, R. I. R. Biyth, M. Mazzeo, M. Anni, G. Gigli and R. Gingolani, *Appl. Phys. Lett.*, 2001, **79**, 560.